

Inhibitor Influence on the Bistability of a CSTR

V. BABUSHOK,* T. NOTO,[†] D. R. F. BURGESS, A. HAMINS,[‡] and W. TSANG

National Institute of Standards and Technology, Gaithersburg, Maryland 20899

Methane combustion in a continuously stirred flow tank reactor (CSTR) in the presence and absence of chemical inhibitors such as CF_3I , CF_3Br , CF_3H , and a chemically inert gas with high heat capacity is simulated with the CHEMKIN program. The aim of the work is to determine the differences in results arising from the use of the various inhibitors with the aim of establishing the capability of CSTR experiments to give a rank ordering of suppressant power. The chemical inhibitors have the general tendency to raise the steady-state temperature. A high heat capacity inert gas leads to the opposite effect. Only near extinction and self-ignition can one obtain a proper scale of flame suppression capability. The curves for combustion efficiency, $(\text{CO}_2/[\text{CO} + \text{CO}_2])$, near the extinction point lead to results where the data for the additives all fall within the envelope for stoichiometric methane/air combustion in the extinction region. For self-ignition, the transition from the mushroom to the isola form of the stability curves appears to be another property that is highly sensitive to suppression power. These observations may serve as a basis for testing inhibition capabilities. Copyright © 1997 by The Combustion Institute

INTRODUCTION

The inhibition of combustion processes are of great practical importance. Currently, there is much interest in finding non-ozone-depleting alternative flame suppressants. Laboratory experiments represent an initial screening alternative to very costly field tests. It is not expected that a single laboratory experiment can capture the myriad of possibilities that occur in actual fire situations. A variety of laboratory tests may, however, mimic some of the elements that are of importance. Combustion phenomena can be studied in premixed flames, plug flow reactors, diffusion flames, static reactors, and continuously stirred flow tank reactors (CSTR). These lead to determinations of various parameters which, at least conceptually, can be related to flame inhibition. These include: flame velocity, ignition delay, reaction time, characteristic concentrations and temperatures, etc. Recent work [1–3] has demonstrated that many of these results can be simulated using chemical kinetic information as a fundamental basis. Such simulations can make laboratory results more meaningful and per-

haps ultimately suggest a suite of tests that will cover a large range of possible fire scenarios.

This paper describes simulation studies in a CSTR with the intention of deducing how results from such studies are affected by the presence of flame inhibitors. Many practical combustion systems can be simulated by a stirred reactor in combination with a plug flow reactor [4]. The former is a particularly useful experimental tool for studying chemical kinetics of high-temperature processes, since mixing problems are eliminated. The present work focuses on how calculations in CSTR systems can match available data on the effectiveness of various inhibitors and suggests how CSTR experiments may be used as a test method. The procedure is to carry out simulations of the oxidation of stoichiometric methane/air mixtures in a CSTR in the presence and absence of known chemical inhibitors such as CF_3Br , CF_3I , and CF_3H as well as a hypothetical chemically inert inhibitor with a large heat capacity. The value of the heat capacity of the chemically inert inhibitor (at the 1% level) was selected in order to obtain the same decrease in flame velocity as a 1% CF_3Br additive. By this means we hope to separate chemical and physical effects. We have recently carried out similar studies in a plug flow reactor configuration and by calculating laminar flame velocities in premixed flames [1, 3]. These results showed that ignition delay times are poor indicators for flame inhibition. On the other hand,

* Guest scientists from Institute of Chemical Kinetics and Combustion, Novosibirsk 630090, Russia.

[†] Guest scientist from NKK Corporation, Kawasaki-Ku, Kawaskai 210, Japan.

[‡] Address for correspondence: A. Hamins, Bldg. 224, Rm B 258, NIST, Gaithersburg, MD 20899.

flame velocity as well as the maximum H-atom concentrations and the reaction time for substantially complete reaction in a plug flow reactor configuration correlate well with known behavior of flame inhibitors.

Experiments in a CSTR are notable in terms of the richness of the phenomena displayed. In such devices it is possible to observe a multiplicity of steady states and different regimes for processes that are nonlinear in character. Transitions between reaction regimes depicted on stationary-state diagrams may form hysteresis loops, mushroom-shaped states, or the isola form [5]. The determination of how different suppressants alter the shape of these curves and the establishment of correlations ranking their relative effect as chemical inhibitors should be extremely interesting.

CHARACTERISTIC BEHAVIOR IN A CSTR

A large literature exists on the analysis of processes taking place in well-stirred reactors [5–7]. A brief physical picture of the behavior of such devices is as follows. The ideal CSTR consists of a vessel with inflow and outflow ducts where complete mixing occurs and therefore reaction processes are controlled by chemical kinetics. In actual practice, these conditions are difficult to achieve and, as seen below, deviations must be considered in the treatment of the results. The flow through the reactor is characterized by a residence time (t_r), or the reactor volume divided by the volumetric flow rate, the ignition delay (t_i), a characteristic reaction time (time for consumption of reactants at a maximum reaction rate, t_{react}), and a characteristic cooling time of the CSTR device (t_q).

Figure 1 contains a qualitative picture of the bistability between high and low temperatures, which are both stable reaction modes. The dependence of the steady-state reaction temperature in the CSTR is shown as a function of flow rate. For initial temperatures below the self-ignition temperature, the situation is illustrated in Fig. 1a. There exist two stable and one unstable solutions (dotted line). It can be seen that the high-temperature mode exists only in the isola state. The region of stable

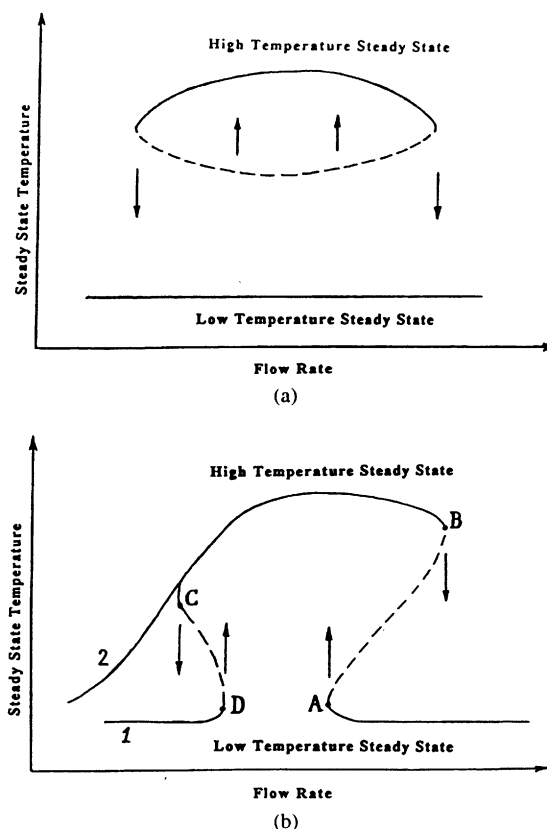


Fig. 1. Qualitative diagram of the steady states and transitions in a CSTR. (a) Isola pattern; (b) 1: mushroom pattern (A, B, C, and D critical points); 2: smooth (noncritical) decrease of a stationary temperature with decreasing flow rate.

combustion (high-temperature mode) is restricted over a wide range of flow rates (residence times) by the influence of heat losses for low values of flow rate and limited consumption of reactants for high values of the flow rate.

At temperatures above the self-ignition temperature, hysteresis loops appear and there can be four critical points (Fig. 1b). Together with the high-temperature stationary states, the left and right hysteresis loops form a mushroom-shaped curve. When initial conditions are changed from a slow reaction by gradually decreasing the flow rate (or increasing the residence time), a jump point (A in Fig. 1b) is ultimately reached. The residence time corresponding to this point is the ignition delay, and transition from low- to high-temperature steady states will occur. Increasing the flow rate at the

high-temperature stationary state leads to the jump point B, where extinction occurs at equal residence and reaction times. Since t_{react} at high temperatures must be less than the ignition delay, the appearance of a right hysteresis loop is observed. With further increases in the residence time, the flow rate becomes the controlling factor in the heat release rate. The left hysteresis loop is the result of competition between the latter and the heat losses from the CSTR. It covers a relatively narrow range of conditions above the self-ignition temperature since, on the high-temperature branch, the reaction rate is higher and the observed transition is for smaller values of the flow rate in comparison to those for the low-temperature branch. With increasing inlet temperature, a smooth decrease of stationary high temperature is observed with decreasing flow rate (Fig. 1b, case 2). Other patterns of behavior can occur in a CSTR. Detailed discussions are found in the literature [5, 7]. In this work, we are concerned with the influence of inhibitors on the right hysteresis loop with the view of establishing a possible basis for experimental studies. It is in this region that most experimental studies are carried out. The calculations for small flow rates were carried out in order to display the complete behavior.

KINETIC MODEL AND MODELING TECHNIQUES

Calculations were carried out using the Sandia CHEMKIN PSR code [8] and analyzed with a NIST interactive graphics postprocessor. The following are some pertinent aspects of the program. The code calculates only the steady-state solutions. There is no possibility of determining the range of parameter values (inlet

temperature, mixture composition, and flow rate) with possible oscillatory (or other non-steady) solutions. Heat-loss effects in the original code, corresponding to a constant rate of heat transfer, are independent of the temperature difference between the reaction vessel and the reacting mixture. This peculiarity leads to decreasing temperature with increasing residence time and to deformed shapes of the mushroom for fixed values of the heat loss. The code was modified to take into account Newtonian-type heat losses depending on the temperature rise. We set the temperature of the reaction vessel as equal to the inlet temperature. The assumed heat transfer coefficient is taken as $1.3 \times 10^{-3} \text{ W/cm}^2 \cdot \text{K}$. Other relevant information can be found in Table 1. For comparison purposes, information on heat-transfer coefficients used in other studies have been summarized. The value of heat loss used here reasonably reproduces the self-ignition temperature of a stoichiometric methane/air mixture at 1 atm (Table 2) and the value of the ignition delay [14, 15]. Increasing the heat-transfer coefficient to twice this value leads to an increase in the self-ignition temperature by approximately 40°C.

The data used in the simulation were based on those for the C/H/O/F system [16] originally developed at NIST for studying the inhibitive effect of fluorinated hydrocarbons. The reactions involving CH_3O_2 and $\text{CH}_3\text{O}_2\text{H}$ have been added because the sequences of reactions involving methyl oxidation are important for methane self-ignition. We have subsequently added reactions involving appropriate bromine and iodine chemistry [2] in order to be able to model systems with CF_3Br and CF_3I . The entire database consists of approximately 1000 reactions with 110 species. Included in the

TABLE 1
Heat Transfer Coefficient

$\alpha, \text{W}/(\text{cm}^2 \text{K})$	Reaction vessel	Reference
1.3×10^{-3}	CSTR, sphere, 200 cm^3	This work
3.28×10^{-3}	Closed stirred and static reactors; cylinder, 1000 cm^3 ; sphere, 800 cm^3	[9]
1.4×10^{-3}	Closed reactor; sphere, 560 cm^3	[10]
$(2-4) \times 10^{-3}$ (recalculation)	CSTR; sphere, 67.4 and 150 cm^3	[11]
2.3×10^{-3}	Stirred closed reactor; sphere, 500 cm^3	[12]
$(1.1-1.8) \times 10^{-3}$	CSTR; sphere, 500 cm^3	[13]

database are the thermodynamic properties of the species. Validation of the database has been made by comparison with experimental measurements. Results can be found in recent publications [1, 2] which contain results on ignition delays and species concentrations as a function of time for the oxidation of H_2 , CH_4 , CH_2O , CH_3OH , and C_2H_6 in the presence and absence of CF_3H , CH_3Br , and CF_3Br . The calculations of the dependence of a steady-state temperature in a CSTR for a high-temperature mode of methane combustion on mixture composition show good agreement with the data [11]. Thus, the general characteristics of the chemistry appear to have been faithfully captured.

RESULTS

Figure 2a and 2b contains the results of simulations of the oxidation of a stoichiometric methane/air mixture in a CSTR for inlet temperatures of 850 and 863 K, respectively. These are directly related to the idealized curves given in Fig. 1. Also included are plots of methane conversion as a function of the mass flow rate. It can be seen that the range of CSTR operations is covered by two stable steady-state regimes, one at low and the other at higher temperatures. At low inlet temperatures, a high-temperature steady-state isola-type solution exists (Fig. 2a). Increasing the inlet temperature extends the range of the isola-type solution. The low-temperature steady-state solution is also raised and the outlet temperature and degree of consumption of initial reactants

are increased. Increasing the inlet temperature until the self-ignition temperature is achieved leads to tangency of the low-temperature steady-state solution and the unstable solution curves at approximately 860 K. Increasing the inlet temperature further leads to the appearance of the left and right hysteresis loops (mushroom), as shown in Fig. 2b. An additional increase of temperature transforms the left hysteresis loop, leading to a smooth decrease of stationary temperature in conformity with Fig. 1b (case 2). Comparisons with numerical calculations for a plug flow reactor demonstrate that the unstable branch of the hysteresis loop approximately reflects the temperature dependence of ignition delay: the residence time at a given temperature for the unstable branch corresponds to the ignition delay for the mixture in the reactor.

Addition of 1% CF_3H , CF_3Br , and CF_3I (individually) to stoichiometric air/methane mixtures leads to an increase in the self-ignition temperature or, equivalently, the need for higher inlet temperatures to effect the transition from isola to hysteresis loop behavior. The general situation is illustrated in Fig. 3. Included in Fig. 3 are the stable branches for the low-temperature steady-state and the unstable branches of the isolas for the systems where three retardants have been added. Thus, addition of inhibitors destroys the mushroom. Indeed, the mushroom shape is not recaptured for the inhibited system until inlet temperatures of 870 K, 1010 K, and 1060 K are reached for CF_3H , CF_3Br , and CF_3I , respectively. This is in contrast to a temperature of 863 K for the

TABLE 2
Self-Ignition Temperature of Methane, 1 atm

References	Temperature, K	Reaction vessel
This work, modeling [9]	860	CSTR; sphere, 200 cm ³
Experiment	885–900	Stirred and static closed vessels; cylinder, 1000 cm ³ ; sphere, 800 cm ³
Modeling [10]	886	Static, closed
Experiment	900	Static closed vessel; sphere, 560 cm ³
Modeling	883	
[14], experiment	873	Closed spherical vessel; sphere, 800 cm ³
[15], experiment	873–882	Closed cylindrical vessel; cylinder, 1200 cm ³

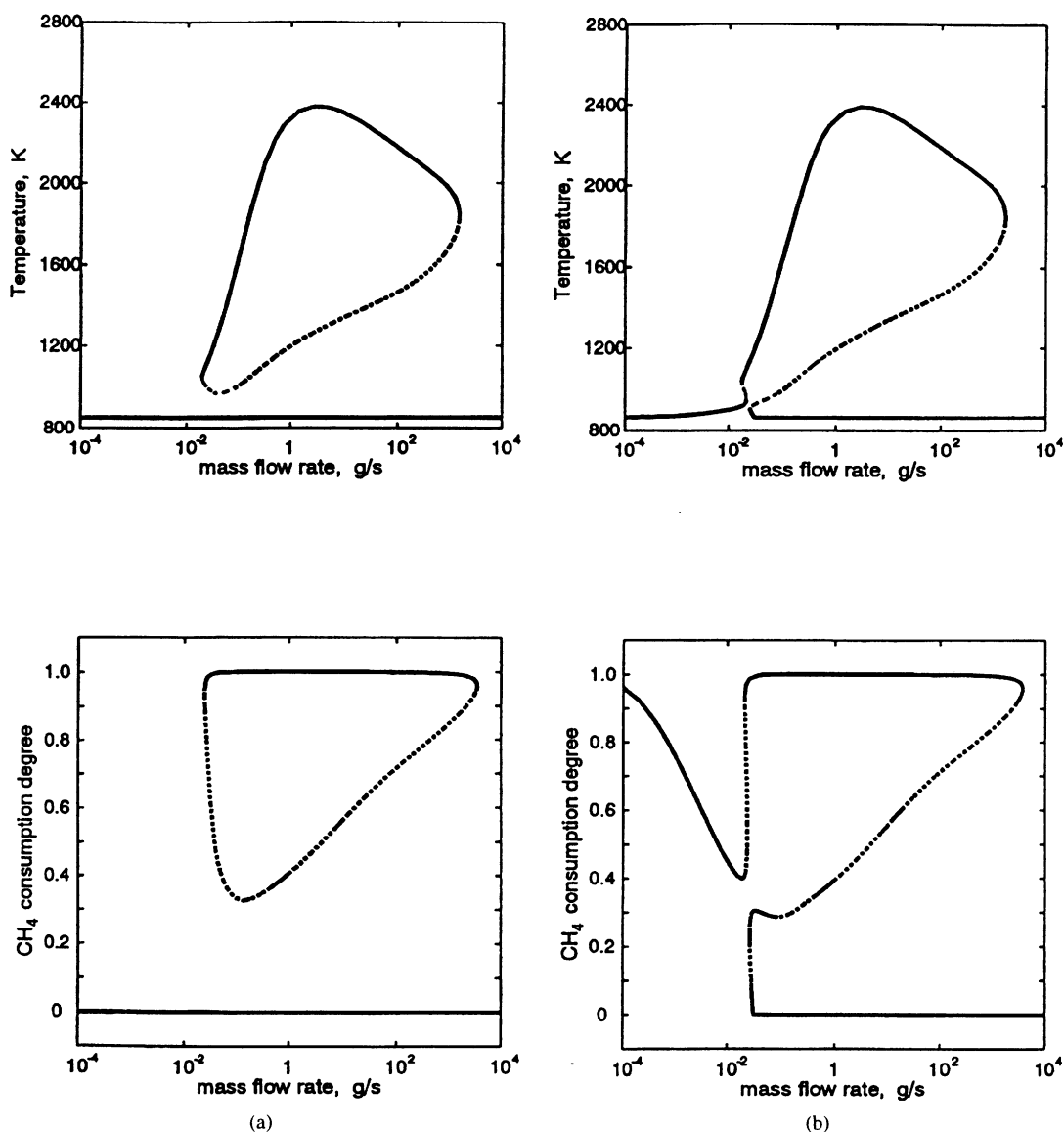


Fig. 2. Stationary-state locus for reaction temperature and degree of methane consumption as function of mass flow rates for a stoichiometric methane/air mixture at 1 atm. Isola (a, 850 K) and mushroom (b, 863 K) cases.

uninhibited system. The results for the inert high capacity additive are also included, and it can be seen that the changes are small.

Figure 4 contains data on the influence of the addition of 1% CF_3I , CF_3Br , and CF_3H on the right hysteresis loop (in terms of mass flow) for an inlet temperature of 1000 K. It can be seen that the three chemical additives all lead to a general shift of the steady states toward higher temperature. Figure 5a and 5b contains

a more detailed look at the self-ignition and extinction points. From Fig. 5a, at 1000 K, it can be seen that, for CF_3I and CF_3Br addition, there are no conditions for self-ignition, and the isola form corresponds to the only possible reaction pathway. This is certainly a manifestation of inhibition. On the other hand, above this temperature (Fig. 6), the addition of inhibitors clearly leads to shorter residence times or an increased mass flow rate. This is equiva-

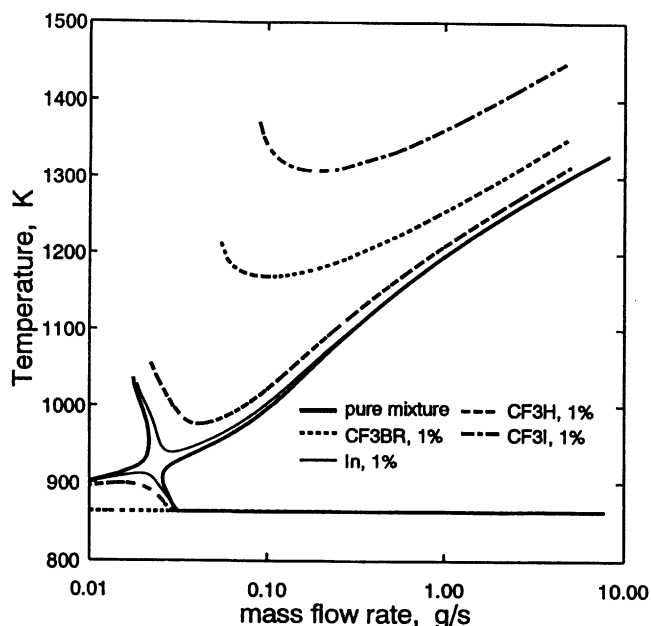


Fig. 3. Detailed picture for ignition point from Fig. 2b. Also included are results on the unstable steady-state curves for with 1% CF_3H , CF_3Br , CF_3I , and chemically inert additive (In) with heat capacity so as to produce the same decrease in flame velocity as 1% CF_3Br . Heat capacity of In was found to be $30 \times C_p(\text{Ar})$. Inlet temperature 863 K.

lent to shorter ignition delays. Thus, the effect of inhibitors in this situation is the opposite of that for the self-ignition temperature. It is, however, consistent with our earlier observations on the promotion effects of the halogenated inhibitors on the ignition delay [1].

Figure 5b shows that the addition of inhibitors leads to longer residence times at the extinction point. However, near the extinction

point, the stationary states for the systems with the additives cross that of the stoichiometric methane/air mixture. Thus, the ordering is lost. On the other hand, for the large heat capacity chemically inert additive that produces the same reduction in burning velocity as CF_3Br , there is a general decrease in the temperature. Thus, the two efforts that are known to increase flame inhibition capability

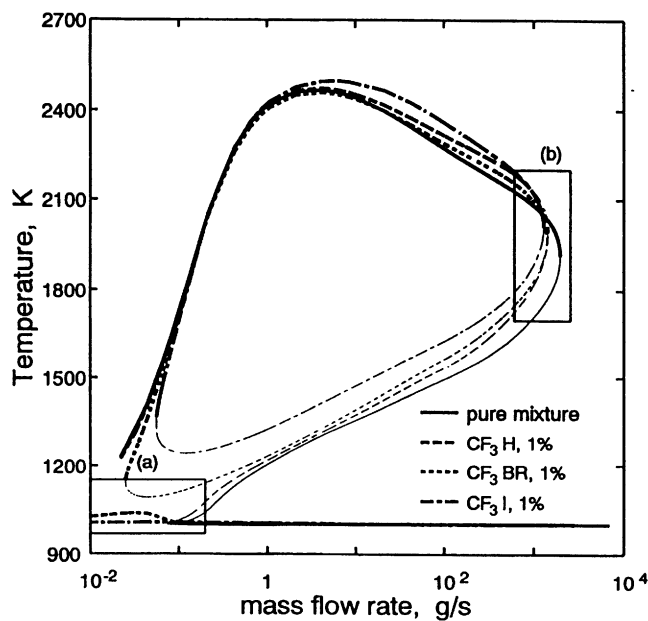
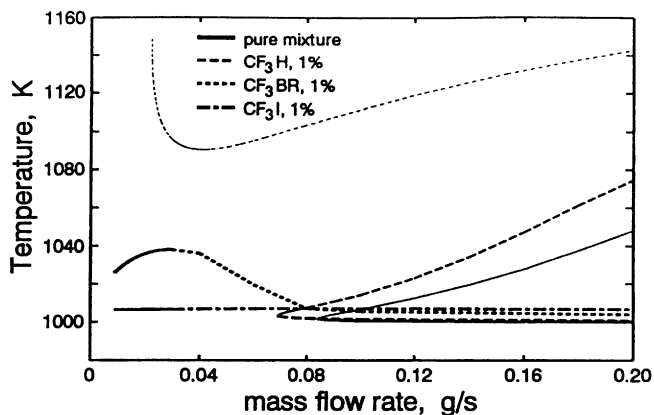
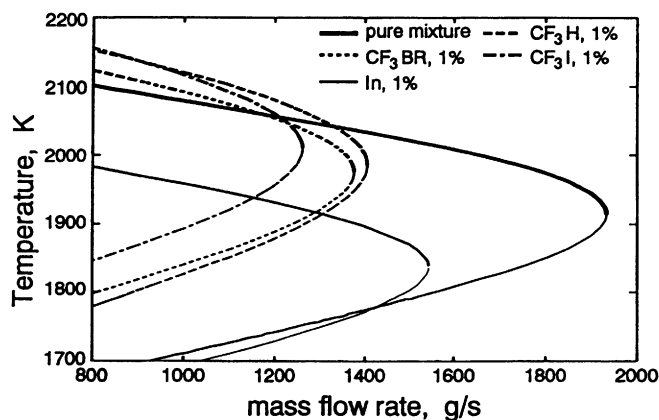


Fig. 4. Dependence of stationary temperature on the flow rate for methane oxidation with 1% CF_3I , CF_3H , and CF_3Br additives at 1000 K and 1 atm for stoichiometric methane/air mixture.



(a)



(b)

Fig. 5. Detailed pictures for ignition (a) and extinction (b) from Fig. 4. Figure 5b contains data for chemically inert additive (In) with a sufficiently large heat capacity so as to produce the same decrease in flame velocity as 1% CF₃Br.

may well cancel each other out in a CSTR experiment.

An alternative way of viewing the data at the extinction point is given in Fig. 7. This contains a plot of the $\text{CO}_2/[\text{CO} + \text{CO}_2]$ ratio near the extinction region. This function is related to

the efficiency of combustion. The stationary states for the stoichiometric methane/air mixture near the extinction point completely overlap those for the system with additives and, on this basis, it is possible to make a rank ordering the effectiveness of the additives.

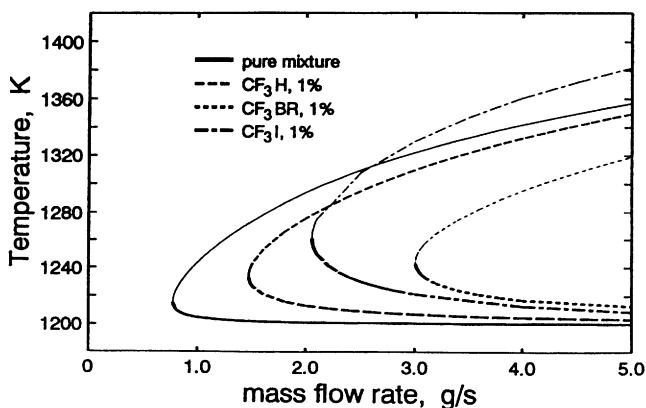


Fig. 6. Additive influence on reaction behavior near ignition point at 1200 K and 1 atm for stoichiometric methane/air mixture and various additives (1%).

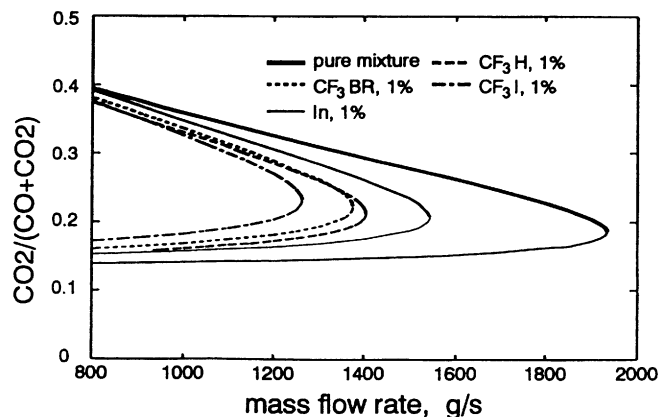


Fig. 7. Stationary-state ratios of $\text{CO}_2/(\text{CO} + \text{CO}_2)$ as a function of mass flow rate in CSTR reactor for pure methane and various additives (1%).

DISCUSSION

The main aim of this work is to use simulations to determine the applicability of the CSTR as a technique to assess flame inhibition capabilities. It is clear that the steady-state temperature is not a satisfactory parameter except at the extinction points. In this region there is a consistent effect as chemical or physical inhibitors are added to the reactive mixture. The general picture is then that of an increased capacity to blow off the high-temperature reaction mode as additives are used. This is equivalent to increased residence time or flame thickness and is in accord with the expected behavior of inhibitors. As one departs from the extinction point, the steady-state solutions for the chemical additives cross the solutions for the pure stoichiometric methane/air mixture and attain higher temperatures. It is possible to attribute this behavior to the decrease in radicals attendant upon the addition of the inhibitors, and hence the need for higher temperatures to maintain the necessary radical concentrations.

Figure 4 shows that the steady-state temperature of the "combustion branch" of the hysteresis loop increases with decreasing mass flow rate from the extinction point until the adiabatic flame temperature is achieved. CH_4 is consumed completely near the extinction point and the consequent increase of temperature is due to the second stage of combustion, or the slow conversion of carbon monoxide to carbon dioxide. Naturally, decreasing the flow rate (increasing the residence time) leads to more complete conversion. Under such conditions,

great sensitivity to inhibition effects are not expected.

The observations on the sensitivity of the self-ignition temperature to inhibition power may be a very important result of this study. Our earlier work has shown that most of the inhibitors reduce the ignition delay time [1, 2]. A very natural assumption is that there must be a direct relation between these two ignition properties. The simulation results suggest that a more careful look at the physical situation is necessary. The following represents some qualitative considerations. Ignition delay measurements are usually carried out in adiabatic systems at temperatures above the self-ignition temperatures. At these high temperatures, promotion effects on the ignition delay are controlled to a considerable extent by the stability (in the unimolecular sense) of the inhibitor. Since these are generally less stable than a fuel such as methane, this represents the first process during the induction period. Ignition near self-ignition conditions occurs at lower temperatures and is at longer times. While contributions from inhibitor decomposition become less important, those from heat loss are more important. The consequence is that an important contributor to ignition behavior is now the steady-state concentration of active species. It is not surprising that the presence of inhibitors would lead to a drastic lowering of radical concentrations and, hence, the need for higher temperatures before ignition occurs. In a sense, the self-ignition temperatures represent a later stage in the reaction process than the ignition delay measurements. We hope to place these concepts on a more quantitative basis in the

near future. For the present, it would appear that there are low- (ignitability) as well as high-temperature (extinction) mechanisms for flame inhibition. A particularly interesting observation is that the low-temperature inhibition effects have apparently a much smaller physical component in comparison to the higher temperature processes.

From this analysis, it is clear that measurements near the critical extinction and self-ignition points are suitable for the determination of inhibition power. A useful measure of the effectiveness of inhibitors in CSTR experiments is the $\text{CO}_2/[\text{CO} + \text{CO}_2]$ ratio. With this parameter, the ordering of the chemical inhibitors is very much in the range that we have previously determined from the criteria for the maximum reaction rate and decrease in flame velocities. Nevertheless, the equivalence of the specific heat and chemical effects for the hypothetical inert high heat capacity additive and CF_3Br as deduced from flame velocity calculations are not reproduced here. The general picture is that of decreasing conversion efficiency as inhibitors are added. Thus measurements of the CO and CO_2 concentrations in a CSTR reactor near the critical extinction points should be a rather straightforward procedure for assessing inhibition efficiency of candidate compounds. The self-ignition temperature measurements can be monitored directly. Conceptually, it can be the basis for a more straightforward test procedure. It is important to note the differences in temperature between the extinction and self-ignition limits. It is very likely that actual chemistry or the radicals of interest may be different and it is important to make the appropriate distinctions. In the present case, CF_3I and CF_3Br seem equally potent under both conditions. An interesting question is whether there may be more specialized compounds in the sense of having effects on only one of the two regions. Finally, it appears that the cup burner test is more comparable to extinction conditions in the CSTR.

The present calculations are all based on an ideal CSTR model without taking into account the physical limitations of a CSTR at small values of residence times for extinction determinations. We suspect that these times are not

realizable in actual practice. In practice, it will probably be necessary to dilute the combustion mixtures. Since the interest is in relative rankings, this probably will not have serious effects on the ordering of the $\text{CO}_2/[\text{CO} + \text{CO}_2]$ ratios. For the ignition temperature, there may be problems with respect to catalysis on the hot walls. Thus, although these simulations do yield extremely suggestive results, many questions remain to be answered by experimentation.

SUMMARY

1. Transition from an isola to a hysteresis loop was obtained for methane combustion in a CSTR. Addition of CF_3I , CF_3Br , and CF_3H increases the inlet temperature necessary for this transition. The transition, which corresponds to the self-ignition temperature, correlates well with suppression power. This is contrary to the ignition delay. Reasons for the differences are presented.
2. In the extinction region, the addition of a chemical inhibitor leads to a general increase in the stationary-state temperature. Physical inhibition (heat capacity) leads to a decrease in the temperature. Only near the extinction point is inhibition manifested through a shifting of the critical point.
3. Combustion efficiency, defined as $\text{CO}_2/[\text{CO} + \text{CO}_2]$, appears to be a satisfactory measure of inhibition. In the vicinity of the extinction point, all results for the inhibitors are overlapped by the data for stoichiometric methane/air mixtures. The ordering and effects from heat capacity and chemistry are all in the expected range.
4. The large differences in temperature between extinction and ignition points suggest that there must be important differences in the dominant chemical processes for inhibition in these regions.

REFERENCES

1. Babushok, V., Burgess, D. R. F., Miziolek, A., Tsang, W., and Miziolek, A., in *Halon Replacements: Technology and Science* (A. Miziolek, and W. Tsang, Eds.), ACE Symposium Series, 1995, vol. 611, pp. 275–288.
2. Babushok, V., Noto, T., Burgess, D. R. F., Hamins, A., and Tsang, W. Accepted for publication in *Combust.*

Flame.

3. Babushok, V., Burgess, D. F. R., Linteris, G., Tsang, W., and Miziolek, A., in *Proc. of Halon Option Technical Conference*, Albuquerque, New Mexico, 1995, pp. 239–249.
4. Brouwer, J., Longwell, J. P., Sarofim, A. F., Barat, R. B., and Bozelli, J. W., *Combust. Sci. Technol.*, 85:87–100 (1992).
5. Gray, P., and Scott, S. K., *Chemical Oscillations and Instabilities*, Clarendon Press, Oxford, 1990.
6. Denbigh, K. G., and Turner, J. C. R., *Chemical Reactor Theory*, Cambridge University Press, Cambridge, 1984.
7. Vulis, L. A., *Thermal Regimes of Combustion*, McGraw-Hill Book Company, New York, 1961.
8. Glarborg, P., Kee, R. J., Grcar, J. F., and Miller, J. A., Sandia National Laboratories Sandia Report No. SAND86-8209, 1986.
9. Reid, I. A. B., Robinson, C., and Smith, D. B., *Twentieth Symposium (International) on Combustion*, The Combustion Institute, Pittsburgh, 1984, pp. 1833–1843.
10. Griffiths, J. F., Coopersthaite, D., Phillips, C. H., Westbrook, C. K., and Pitz, W. J., *Twenty-Third Symposium (International) on Combustion*, The Combustion Institute, Pittsburgh, 1990, pp. 1745–1752.
11. Glarborg, P., Miller, J. A., and Kee, R. J., *Combust. Flame*, 65:177–202 (1986).
12. Griffiths, J. F., Gray, P., and Kishore, K., *Combust. Flame*, 22:197–207 (1974).
13. Di Maio, F. P., Lignola, P. G., and Talarico, P., *Combust. Sci. Tech.*, 91:119–142 (1993).
14. Robinson, C., and Smith, D. B., *J. Hazardous Materials*, 8:199–203 (1984).
15. Conti, C. R., and Hertzberg, M., *J. Fire Sci.*, 6:348–355, (1988).
16. Burgess, D. R. F., Jr., Zachariah, M. R., Tsang, W., and Westmoreland, P. R., NIST Technical Note No. 1412, Washington DC, 1995.